This manuscript was published as formal in:

International Journal of Biological Macromolecules 2021, 193, 2021, 414-424

DOI: 10.1016/j.ijbiomac.2021.10.174

https://doi.org/10.1016/j.ijbiomac.2021.10.174

***Title*:**

Amphiphilic chitosan-g-poly(trimethylene carbonate) – A new approach for biomaterials design

Bianca-Iustina Andreica[1], Daniela Ailincai[1], Andreea-Isabela Sandu[1], Luminita Marin[1]*

[1]"Petru Poni" Institute of Macromolecular Chemistry of Romanian Academy, Iasi, Romania

*email: lmarin@icmpp.ro

Abstract

The paper presents the synthesis and characterization of poly(trimethylene carbonate) grafted chitosan as a new water soluble biopolymer suitable for *in vivo* applications. The synthesis was performed *via* ring-opening polymerization of 1,3-dioxan-2-one (trimethylene carbonate) (TMC) monomer, initiated by the functional groups of chitosan in the presence of toluene as solvent/swelling agent. By varying the molar ratio between the glucosamine units of chitosan and TMC, a series of chitosan derivatives with different content of poly(trimethylene carbonate) chains was synthetized. The structural characterization of the polymers was realized by FTIR and ^{1}H-NMR spectroscopy and their solubility was assessed in water and in organic solvents as well. The biocompatibility was investigated by MTS assay on Normal Human Dermal Fibroblasts, and the biodegradability was evaluated in lysozyme buffer solution. Further, the surface properties of the polymer films were analyzed by polarized optical microscopy, atomic force microscopy and water-to-air contact angle measurements. It was established that, by 5% substitution of chitosan with poly(trimethylene carbonate) chains having an average polymerization degree of 7, a water soluble polymer can be attained. Compared to the pristine chitosan, it has improved biocompatibility in solution and moderate wettability and higher biodegradability rate in solid state, pointing its suitability for *in vivo* applications.

Keywords: chitosan; poly(trimethylene carbonate); water soluble; biocompatibility; biodegradability;

1. Introduction

Chitosan is a natural originated biopolymer which fulfills the main requirements for *in vivo* applications, biocompatibility and biodegradability, and it shows attractive bioactive properties, such as antimicrobial, immunoadjuvant and hemostatic activity, ability to form protective films and coatings, to selectively bind acidic liquids lowering serum cholesterol levels, to favor the wound healing and tissue regeneration and to chelate metals [1-4]. In the light of these valuable properties, chitosan has attracted a tremendous research interest focused on creating new ecological materials for applications of contemporary interest in biomedicine, environmental protection and agriculture [5-13]. However, the use of chitosan for biomedical field is restricted by its low solubility in media with pH above 6.5, mainly correlated with the strong network of intra- and inter-molecular H-bonds [2]. To overcome this disadvantage, the point of interest of

researchers was the chemical modification of chitosan, either at the amine or hydroxyl groups. This not only emancipates the amine and hydroxyl groups from the H-bonding network, but also could endow chitosan with new functions [14-19]. Over time, many functional groups were used to achieve this goal: carboxyalkyl [21,22], sulfate [23], alkyl [24], poly(ethylenglycol) [5], thiolate [25], phosphate [26], quaternary ammonium salts [27]. The resulted chitosan derivatives presented promising advantages for specific applications, encouraging further exploration of new chitosan derivatives [27-29].

In this line of thought, the goal of this paper was the synthesis of novel water-soluble chitosan derivatives, by grafting poly(trimethylene carbonate) (PTMC) chains on the chitosan backbone, *via* ring-opening polymerization (ROP) technique. The design of these polymers took into consideration that PTMC meets the requirements for *in vivo* applications, being biocompatible and biodegradable. Besides, its enzymatic degradation leads to non-acidic products and lack of toxicity for living organisms [30]. Due to these features, PTMC is used for soft graft materials in tissue regeneration, and as hydrophobic segment of amphiphilic copolymers for drug delivery [31, 32]. Its use for biomedical applications presents two main advantages: the slow degradation rate leading to a longer lifespan of medical devices and the non-acid degradation reducing the risk of adverse *in vivo* reactions. These premises led us to the idea that the combination of chitosan with PTMC has good chances to generate new multifunctional biopolymers with valuable properties for *in vivo* applications. Thus, the aim of the paper was the synthesis of PTMC-grafted-chitosan and the investigation of the properties required for *in vivo* applications.

2. Experimental

2.1 Materials

Low molecular weight chitosan was purchased from Sigma-Aldrich and dried before use, *in vacuum*, for 48 hours at 80 °C and 0 mbar. Its molecular weight was calculated by measuring the viscosity with an Ubbelohde type viscometer based on Mark–Houwink equation (197 kDa), and the degree of acetylation (DA=16%) was determined from ^{1}H-NMR (see Figure S1, Figure S2 in Supporting Information). Trimethylene carbonate purchased from ActuAll Chemicals was dried *in vacuum* at 0 mbar for 2 hours before use. Toluene and ethanol (Sigma-Aldrich) were dried overnight on 3 Å molecular sieves, previously activated in an oven at 200 °C, 0 mbar, for 2 hours. Lysozyme from Sigma Aldrich (lyophilized powder, protein 90%, 40,000 units/mg protein) and all other solvents were of analytical grade, and used as received.

NHDF cells were purchased from PromoCell (Heidelberg, Germany), Eagle's Minimal Essential Medium alpha (aMEM) and Penicillin–Streptomycin–Amphotericin B mixture (10000 units/mL - 10000 µg/mL - 25 µg/mL) from Lonza (Verviers, Begium), fetal bovine serum (non-USA origins) from Sigma Aldrich (Schnelldorf, Germany), TrypLE™ Express Enzyme from Gibco (Langley, VA, USA), phosphate buffered saline (PBS) from Invitrogen (Eugene, OR, USA), CellTiter 96® Aqueous One Solution Cell Proliferation Assay (MTS) from Promega (Madison, WI, USA), CytoOne® 96-well plates from StarLab (Hamburg, Germany).

2.2 Equipment and methods

The *lyophilization* was done with a freeze dryer equipment (LABCONCO FreeZone Freeze Dry System), at -50 °C, 1.510 mbar, for 24 hours. The aqueous solutions of samples were previously frozen in liquid nitrogen.

The structural characterization of the compounds was performed using the Bruker Vertex 70 *FT-IR* spectrophotometer equipped with ATR accessory (Ettligen, Germany) and Bruker Avance DRX 400 MHz *NMR* spectrometer. The degree of polymerization (DP) of poly(trimethylene carbonate) was calculated from the ratio between the methylene protons from the repeating unit (–O–CH_2–C<u>H</u>$_2$–CH_2–O–) and the methylene protons from the end group (-CH_2–C<u>H</u>$_2$–OH or -C<u>H</u>$_2$–CH_2–OH) given by the integrated intensity of their signals. The grafting degree of chitosan with PTMC chains was roughly estimated considering the integrated intensity value of the chemical shift of the methylene protons in repeating unit (–O–CH_2–C<u>H</u>$_2$–CH_2–O–) and that of the acetyl unit (–NH–CO–C<u>H</u>$_3$) of chitosan.

The supramolecular organization of the new products was assessed from the polarized optical microscopy (*POM*) images acquired with a Leica DM 2500 microscope.

Atomic force microscopy (*AFM*) images were acquired on thin films, using an Ntegra Spectra instrument at room temperature, in semi-contact mode, using a cantilever of silicone (NSG 10). The thin film samples were prepared by casting a 1% solution of polymer on glass lamellae. Nova v.1443 software was used to record and to analyze the AFM topographic images.

The *water-to-air contact angle* measurements were done by the sessile drop method, within 10 s after placing 1 µL drop of water on the film surface, using a CAM-200 instrument (KSV- Finland). The films were prepared by casting 1% polymer solutions on glass lamellae. Contact angle measurements were taken 5 times at different locations on the film surface, the average value being considered and expressed as average ± standard deviation.

The *solubility* of the obtained copolymers was firstly assessed visually, for concentrations of 1% in water and in organic solvents, such as: methanol, dimethyl sulfoxide and dimethylformamide. The products which showed macroscopic transparent solutions in water were further investigated for pH-dependent solubility, monitoring the solutions' transmittance by UV–Vis spectroscopy on a Perkin Elmer Lambda 35 *UV-Vis* spectrophotometer (Paris, France) [33] and the formation of nanoparticles by *DLS* (Delsa Nano C, Beckman Coulter (United States)). Pristine chitosan was used as reference. For pH-dependent solubility measurements, the samples were firstly dissolved in water at two concentrations, 0.5 mg/mL and 1 mg/mL, and then the pH was adjusted to 3 with glacial acetic acid and subsequently increased up to 9 with 1M NaOH. The maximum transmittance and nanoparticles' formation was monitored for each solution.

The *biocompatibility* was determined by evaluation of the viability of Normal Human Dermal Fibroblasts (NHDF) in contact with films or solutions of the samples of different concentrations, by MTS assay.

For determination of biocompatibility in solution, 1% stock solutions of grafted chitosan derivatives in ultrapure water and 1% stock solutions of chitosan in 1% acetic acid were firstly prepared. The stock solutions were diluted ten times in culture medium to obtain working solutions, thus, the maximum concentration of acetic acid was 0.1%. The working solutions were then further diluted in culture medium to reach concentrations of 25, 50, 100, 300 and 400 µg/mL. Cells were cultivated in complete Eagle's Minimal Essential Medium alpha (aMEM) containing 1% Penicillin/Streptomycin/Amphotericin B mixture and 10% fetal bovine serum under 5% CO_2 humidified atmosphere, at 37 °C. TrypLE^{TM} Express Enzyme was used for passaging cells. Negative control cells were treated only with complete cell culture medium. In order to perform the MTS assay, cells were placed in 96-wells plates at densities of 5 x 10^3 cells/well for NHDF cell line in 100 µL aMEM medium/well and incubated for 24 hours. After 24 h, the media was replaced with the tested compounds solutions at various concentrations (25, 50, 100, 200, 300 and 400 µg/mL) and the plates were incubated for another 48 hours. Next, 20 µL MTS solution/well was added and the plates were incubated for 3 hours. Finally, the absorbance at $\lambda = 490$ nm was recorded with a microplate reader. The relative cell viability was expressed as percentage of the viability of control (cells treated only with cell culture medium). The absorbance for CellTiter 96® Aqueous One Solution Cell Proliferation Assay (MTS) was measured with FLUOstar Omega Filter-based multi-mode microplate reader from BMG LABTECH (Offenburg, Germany). Data analysis was performed with GraphPad Prism

software version 7.00 for Windows (GraphPad Software, San Diego, CA). The obtained results represent the mean ± standard error of the mean (S.E.M.) of three different experiments.

Cytotoxicity of films was assessed by MTS assay using the CellTiter 96® AQueous One Solution Cell Proliferation Assay (Promega, Madison, WI USA), according to the manufacturer instructions and direct contact procedure adapted from ISO 10993-5:2009(E). The films were prepared into 24-well plates by adding 20 µL solution containing 150, 50 and 12.5 µg of sample and dried overnight under vacuum for solvent removal. Normal fibroblasts were seeded over the films, at a density of 3.5×10^4 cells/well in 500 µL aMEM medium/well and incubated for 48 hours. The final amount of compounds in medium was: 300, 100 and 25 µg/mL. Control cells were incubated only with culture medium. Prior to absorbance reading, the medium was removed and fresh medium and MTS reagent were added and incubated for 1-3h. After the formazan's formation, a triplicate of each homogeneous solution was transferred into a 96-well plate, and the final reading was performed at 490 nm on a FLUOstar® Omega microplate reader (BMG LABTECH, Ortenberg, Germany). Experiments were done in triplicate and treated cells viability was expressed as percentage of control cells' viability. Graphical data were expressed as means ± standard error of the mean (S. E. M.).

Statistical analysis was performed with GraphPad Prism 7 using two-way ANOVA followed by Dunnett's multiple comparisons test. The difference was considered significant when $p < 0.05$.

The *in vitro enzymatic degradation* was assessed quantitatively by determination of the mass loss of the chitosan derivatives kept in lysozyme buffer solution (pH = 7.4) at 37 ^{o}C, for 21 days. Pieces of samples of known weight were immersed in lysozyme solution in PBS (10 mg/L) to give the concentration of 1 mg/mL. Every three days, the lysozyme solution was removed and replaced with freshly prepared one [34]. After 21 days, the pieces were taken off, washed three times with distilled water to remove the PBS salts, lyophilized, and analyzed by weighting and by SEM technique. The biodegradation was assessed by calculating the mass loss using the equation W_{loss} (%) = $[(W_i - W_f) / Wi] \cdot 100$, where W_{loss} = the percent of loss sample, W_i = the initial weight of the sample, and W_f = the final weight of the sample.

The microstructure of the compounds before and after biodegradation was investigated with a field emission Scanning Electron Microscope SEM EDAX – Quanta 200, operated at 20 keV accelerating voltage.

2.3 Synthesis

The synthesis of the PTMC-grafted-chitosan derivatives was realized by ring-opening polymerization reaction of 1,3-dioxan-2-one (trimethylene carbonate) (TMC) monomer

initiated by the functional groups of chitosan. To establish the synthetic procedure for the targeted polymers, different reaction conditions were tested, such as (i) varying the molar ratio between glucosamine units of chitosan and TMC, (ii) the presence/absence of $Sn(Oct)_2$ catalyst, and (iii) the presence/absence of toluene solvent as chitosan's swelling agent. The synthesis of PTMC homopolymer was carried out in similar conditions, in order to create a reference useful for the interpretation of characterization data of PTMC-grafted-chitosan derivatives. For PTMC synthesis, ethanol was used as initiator. A short overview of the synthetic trials was given in Scheme 1. The products were coded considering the principal building blocks of copolymers: (i) chitosan (**C**) and poly(trimethylene carbonate) (**P**); (ii) the molar ratio between TMC and initiator (ethanol or glucosamine in the case of chitosan (TMC/ethanol or TMC/glucosamine); (iii) the presence of $Sn(Oct)_2$ catalyst (**S**) or toluene (**T**). *E.g.* the polymer prepared by reacting TMC with chitosan in 20/1 molar ratio of TMC/glucosamine, in the presence of $Sn(Oct)_2$ was coded **PC-20-S**, while the polymer prepared by reacting TMC with ethanol initiator in 20/1 molar ratio, in the presence of $Sn(Oct)_2$ was coded **P-20-S**.

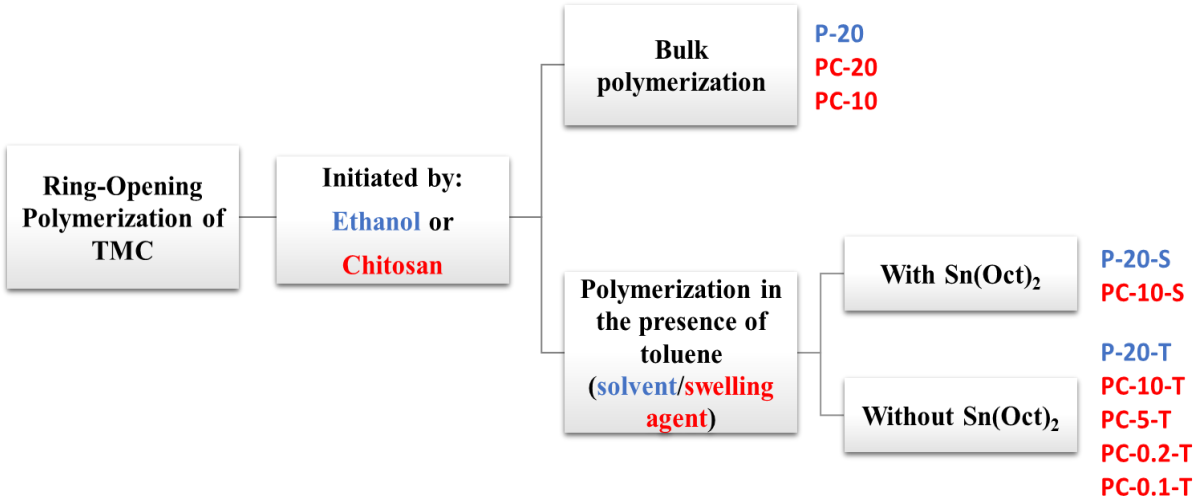

Scheme 1. Representation of the synthetic strategies and the codes of the obtained polymers

The synthesis of chitosan derivatives followed the same procedures as in the case of the PTMC homopolymers (see Supporting Information, including Figures S3-S8), being performed in melt bulk or in heterogeneous media, when toluene was used as swelling agent of chitosan. **PC-20:** The **PC-20** chitosan derivative was synthesized in melt bulk, for a TMC/glucosamine molar ratio of 20/1 (200 mg TMC, 16.5 mg chitosan), according to **P-20** receipt [35]. TMC was charged into a previously heated Schlenk tube attached to a Schlenk line, and heated under vigorous magnetic stirring at 60 °C under nitrogen atmosphere until the monomer was completely melted. Further, it was subjected to three cycles of vacuum/nitrogen purge in order

to assure a water-free atmosphere, and it was cooled at room temperature. Chitosan was then added under nitrogen flow, and the reaction tube was subjected to the degassing process (three vacuum/nitrogen purge cycles). The reaction tube was fitted with a reflux condenser and immersed in a preheated oil bath at 120 °C, under nitrogen flow and continuous stirring. Chitosan formed an obvious heterogeneous mixture with the melted monomer. After 24 hours, chloroform (10 mL) was added, the solid was separated by filtration, and the solution was re-precipitated in cold diethyl ether and then centrifuged to give a white, waxy solid. FTIR spectrum of the solid product separated by filtration showed intense vibration bands characteristic for PTMC and low intensity vibration bands characteristic for chitosan (Figure S9), but its low solubility in deuterated solvents hampered its proper analysis by NMR spectroscopy. FTIR and NMR analysis of the white, waxy solid obtained after re-precipitation showed characteristic bands for PTMC, with a DP = 22.

FTIR (ATR, cm^{-1}): 3635-3396 ($\upsilon_{OH,}$ υ_{Hbonds}), 2971, 2909 (υ_{C-H}), 1744 ($\upsilon_{C=O}$), 1586 ($\upsilon_{N-H\ amide}$), 1332 ($\upsilon_{C-N\ amide}$), 1245 (υ_{C-O}) (Figure S9).

PC-10: In order to avoid the disadvantages of a low amount of chitosan and a low contact between reagents, the reaction protocol has been adjusted, as follows. TMC (100 mg, 0.98 mmol) and chitosan (16.5 mg, 0.098 mmol) (TMC/glucosamine molar ratio =10/1) were previously grinded together into an agate mortar with a pestle. Then, the obtained mixture was charged into a degassed Schlenk tube, and further the procedure for **PC-20** obtaining and purification was applied, leading to similar results, with the only difference of a lower polymerization degree for PTMC (DP=16). It was concluded that these conditions were did not help to surpassing the disadvantage of a low contact between reagents and were not favorable for the grafting of PTMC on chitosan.

FTIR (ATR, cm^{-1}): 3693-3253 ($\upsilon_{OH,}$ υ_{Hbonds}), 2970, 2920, 2854 (υ_{C-H}), 1736 ($\upsilon_{C=O\ carbonate}$), 1228 ($\upsilon_{C-O\ carbonate}$), (Figure S10).

PC-10-S: The synthesis was performed according to the **PC-10** receipt, with the only difference of using $Sn(Oct)_2$ as catalyst, similar to **P-20-S** (see Supporting Information). Chitosan (165 mg, 0.98 mmol) and TMC (1 g, 9.8 mmol) were added into a Schlenk tube, under inert nitrogen atmosphere and continuous stirring. In the first step, the synthesis was maintained at 60 °C for 2 hours, and then a solution of $Sn(Oct)_2$ (3 µL $Sn(Oct)_2$ in 16 mL toluene) was added to the reaction mixture. The temperature was increased to 100 °C and kept constant for 24 h. The reaction mixture was diluted with toluene, the solid was filtered and the solution was lyophilized. FTIR and NMR analysis indicated similar results as for **PC-10**.

FTIR (ATR, cm^{-1}): 3718-3066 (υ_{OH}), 2969, 2912 (υ_{C-H}), 1739 ($\upsilon_{C=O}$), 1233 ($\upsilon_{C-O\ carbonate}$), 1026, 913, 786 ($\upsilon_{C-C}$), (Figure S11).

PC-10-T: To favor a better contact between chitosan and TMC, the synthesis was performed in toluene solution, similar to **P-20-T** receipt, with slight modifications [36]. TMC (100 mg, 0.98 mmol) was added into a Schlenk tube and dissolved in 1.65 mL toluene under N_2 purge for 15 minutes. Chitosan (16.5 mg, 0.098 mmol) was added to the solution and the reaction temperature was gradually increased to 100 °C (with 10 degrees every 15 minutes), and the synthesis was allowed to proceed for 22 hours. Then, the reaction medium was filtered, and the precipitate was washed with toluene and dried *in vacuum* at 80 °C, while the liquid fraction was lyophilized. Both products were subjected to FTIR and NMR analysis (Figure S12,S13), which demonstrated that the solid was chitosan grafted with poly(trimethylene carbonate) (DP=7) and the solid collected from solution was unreacted TMC. Considering the integrated intensity of the chemical shift corresponding to the protons of acetyl unit of chitosan, the grafting degree of the **PC-10-T** was roughly estimated around 5%. η=16.7%

^{1}H-NMR (400.13 MHz, D_2O, ppm): δ = 4.48 (t, 4x6.26H, -O-$\underline{CH_2}$-CH_2-$\underline{CH_2}$-O-), 3.88-3.15 (H_2-H_6 from chitosan), 3.62 (t, 2H, -$\underline{CH_2}$-OH), 2.02 (m, 2x7.09H, -O-CH_2-$\underline{CH_2}$-CH_2-O-), 2.11 (s, 3x3.33H, H_{acetyl}), 1.75 (m, 2H, -$\underline{CH_2}$-CH_2-OH) (Figure S12).; FTIR (ATR, cm^{-1}): 3701-3036 ($\upsilon_{OH,}$ $\upsilon_{NH,}$ $\upsilon_{H\ bonds}$), 2922, 2859 (υ_{C-H}), 1739 ($\upsilon_{C=O\ carbonate}$), 1650 ($\upsilon_{C=O\ amide}$), 1591 ($\upsilon_{N-H\ amide}$), 1251 ($\upsilon_{NHCO}$, $\upsilon_{C-O\ carbonate}$), 1188 ($\upsilon_{C-O-C\ chitosan}$), 1029 ($\upsilon_{C-O\ chitosan}$) (Figure S13).

PC-5-T: The synthesis was performed in similar conditions as **PC-10-T**, decreasing the TMC/glucosamine molar ratio to 5. FTIR of the solid fraction demonstrated the successful grafting, but the product was not soluble either in organic solvents or in water, making the NMR spectra recording impossible. η=16.9%; FTIR (ATR, cm^{-1}): 3696-3015 ($\upsilon_{OH,}$ $\upsilon_{NH,}$ υ_{Hbonds}), 2922, 2854 (υ_{C-H}), 1744 ($\upsilon_{C=O\ carbonate}$), 1651 ($\upsilon_{C=O}$ amide), 1591 (υ_{N-H}), 1259 (υ_{NHCO}, $\upsilon_{C-O\ carbonate}$), 1151 ($\upsilon_{C-O-C\ chitosan}$), 1062, 1025 ($\upsilon_{C-O\ chitosan}$) (Figure S14).

PC-0.2-T: The chitosan derivative was synthesized according to the same procedure, only decreasing more the TMC/glucosamine molar ratio to 0.2 (24 mg TMC, 200 mg chitosan). FTIR spectrum showed the vibration bands characteristic to the grafted chitosan. The product was soluble in acidic aqueous solution. Interesting, the NMR spectrum showed the chemical shift of the chitosan protons and the chemical shift of the methylene group protons neighbor to the hydroxyl from the PTMC but not the protons characteristic to the PTMC repeating units, suggesting that small oligomers or rather only one unit of TMC were grafted. η=84.82%

^{1}H-NMR (400.13 MHz, D_2O+HCl, ppm): δ = 3.87-3.13 (H_2-H_6), 3.62 (m, 2H, -CH_2-CH_2-$\underline{CH_2}$-OH), 2.01 (s, 3x5.33H, H_{acetyl}) (Figure S15).; FTIR (ATR, cm^{-1}): 3706-3048 ($\upsilon_{OH,}$ $\upsilon_{NH,}$ υ_{Hbonds}),

2964, 2923, 2856 (υ_{C-H}), 1742 ($\upsilon_{C=O\ carbonate}$), 1654 ($\upsilon_{C=O}$ amide), 1584 (υ_{N-H}), 1243 ($\upsilon_{NHCO,}$ $\upsilon_{C-O\ carbonate}$), 1149 ($\upsilon_{C-O-C\ chitosan}$), 1026 ($\upsilon_{C-O\ chitosan}$) (Figure S16).

PC-0.1-T: The compound was synthetized according to the same receipt, decreasing more the amount of TMC to 1/10 TMC/glucosamine molar ratio (6 mg TMC, 100 mg Chitosan). The product was soluble in neutral water. The FTIR spectrum was similar with those of the other PC derivatives, but with significant lower intensity of the bands characteristic to the carbonate group. The ^{1}H-NMR spectrum showed similar chemical shifts with **PC-0.2-T**. η=90.5%

^{1}H-NMR (400.13 MHz, D_2O, ppm): δ = 3.88-3.14 (H_2-H_6), 3.62 (m, 2H, -CH_2-CH_2-$\underline{CH_2}$-OH), 2.05 (s, 3x5.33H, H_{acetyl}), (Figure S17).; FTIR (ATR, cm^{-1}): 3700-3009 ($\upsilon_{OH,}$ $\upsilon_{NH,}$ υ_{Hbonds}), 2922, 2855 (υ_{C-H}), 1742 ($\upsilon_{C=O\ carbonate}$), 1649 ($\upsilon_{C=O\ amide}$), 1587 ($\upsilon_{N-H}$), 1254 ($\upsilon_{NHCO,}$ $\upsilon_{C-O\ carbonate}$), 1150 ($\upsilon_{C-O-C\ chitosan}$), 1062, 1025 ($\upsilon_{C-O\ chitosan}$), (Figure S18).

3. Results and discussions

3.1 Synthesis and characterization

New chitosan derivatives were synthetized by grafting PTMC chains on the chitosan backbones by ring-opening polymerization of TMC, initiated by the functional groups of chitosan. Various reaction conditions were applied with the aim to reach chitosan derivatives with good solubility in aqueous solutions, suitable for *in vivo* applications. The synthesis of PTMC in similar conditions was also performed using ethanol as initiator, in order to create a data set useful for understanding the synthetic pathway and for an accurate interpretation of the characterization data. The modifications of reaction conditions consisted in the variation of molar ratio between TMC monomer and initiator, the presence/absence of $Sn(Oct)_2$ as catalyst and the presence/absence of toluene as reaction medium. The synthetic pathways, the codes of the synthetized polymers, the polymerization degrees and the polymers' structures were given in Scheme 2.

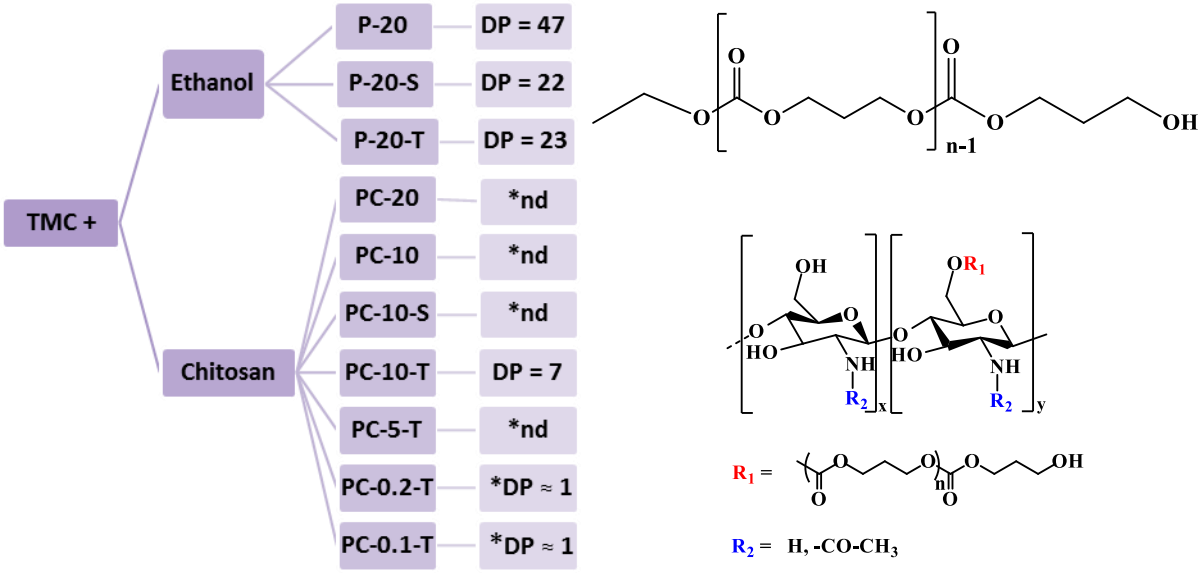

Scheme 2. Representation of the synthetic routes for the obtaining of PTMC-grafted-chitosan derivatives and PTMC reference homopolymers and their polymerization degree (DP). The products' codes reflect the composition and reaction conditions, i.e. the number is the value of TMC/initiator molar ratio; **S** - reflects the presence of $Sn(Oct)_2$ catalyst; **T**- reflects the presence of toluene. *DP – polymerization degree assessed based on correlative information; *nd - not determined because of the compound's insolubility.

FTIR spectra confirmed the successful synthesis of the grafted chitosan by the presence of the absorption bands characteristic to chitosan and PTMC, i.e. the vibration of C=O (~1740 cm^{-1}) and C-O (~1225 cm^{-1}) bonds of carbonate groups of PTMC [35, 36], and the vibrations characteristic to C=O (1650 cm^{-1}), N-H (1591 cm^{-1}) and C-O (1029 cm^{-1}) bonds of amide units of chitosan (Figure 1) [18]. All other bands characteristic for PTMC and chitosan were present too, suggesting that the reaction conditions did not inflict side chemical transformations. The intensity of the absorption bands was in accordance with the ratio between PTMC and chitosan components. These spectroscopic evidences along with the modification of physico-chemical properties (color, aspect, and solubility) supported the conclusion of successful grafting reaction.

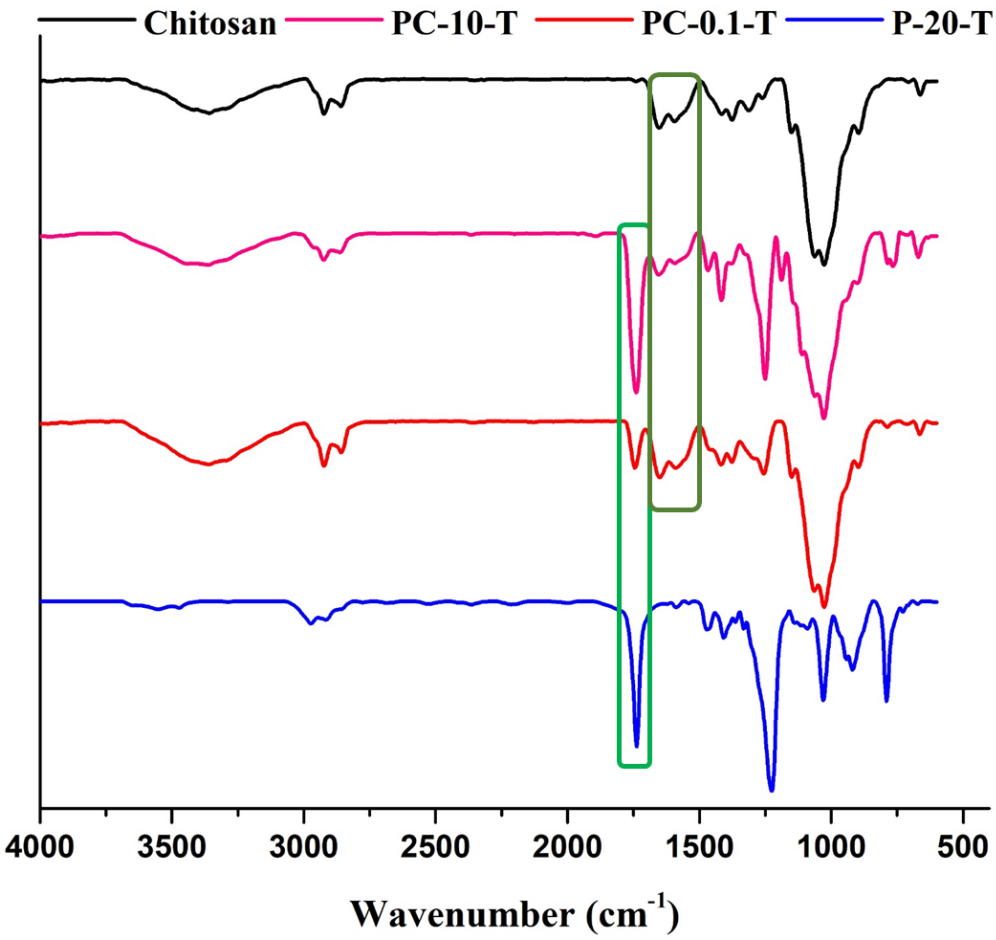

Figure 1. FTIR spectra of the **PC-10-T** and **PC-0.1-T** PTMC-grafted-chitosan derivatives, compared to **chitosan** and **P-20-T** references

Moreover, the ^{1}H-NMR spectra of the products with proper solubility in water or in organic solvents supported the FTIR data and brought information regarding the polymerization degree of PTMC and grafting degree of chitosan (see the Experimental part and Supporting Information). The ^{1}H-NMR spectra displayed the chemical shifts of H2-H6 protons from chitosan (from 3.88 to 3.15 ppm), and the chemical shifts of the protons of repeating unit (4.48 and 2.16 ppm) and end groups (3.62 and 1.75 ppm) from PTMC (Figure 2). The ratio between the integrated intensity of the chemical shifts of the protons from repeating units and end groups allowed a rough estimation of the PTMC polymerization degree (Scheme 2). Further, the ratio between the integrated intensities of the chemical shifts of PTMC end group protons and acetyl group protons of chitosan allowed the estimation of the grafting degree of chitosan. It was assessed that the water soluble **PC-10-T** derivative consisted of chitosan backbones 5% substituted with PTMC chains with DP=7.

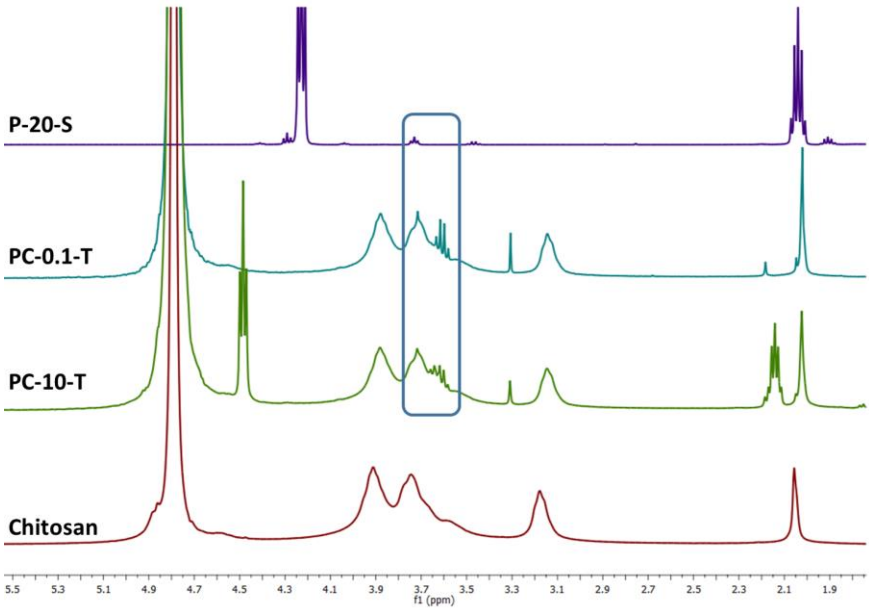

Figure 2. ^{1}H-NMR spectra of **PC-10-T** and **PC-0.1-T** grafted chitosan derivatives, compared to **chitosan** and **P-20-T** references (The slight shifting of the bands resulted due to the different deuterated solvents used for NMR recording)

Interesting enough, when a small amount of TMC was used as reagent (**PC-0.2-T**, **PC-0.1-T**), the chemical shifts characteristic to chitosan's protons, from 3.88 to 3.1 ppm, were superposed with a multiplet around 3.7 ppm characteristic to the protons neighbor to the hydroxyl group of PTMC end group. No other signals were discriminated in the spectra. Taking into consideration that FTIR spectra presented the characteristic bands for carbonate and amide groups of two building blocks of the PTMC-grafted-chitosan, we hypothesized that only TMC units bonded to the chitosan backbone and not PTMC chains, and developed non-classical inter-molecular H-bonds with the neighbor hydroxyl groups [37], causing the nuclei "deshielding" and consequently shifting the peak downfield [38, 39].

Literature data shows that ring-opening polymerization of TMC to give PTMC is affected by the TMC/initiator ratio and reagents' purity and less by the presence of the catalyst [40]. Nevertheless, we observed that in the case of bulk TMC polymerization using ethanol as initiator, $Sn(Oct)_2$ catalyst induced a lower polymerization degree of 22 *versus* 47 (Scheme 2). A similar diminishing of the polymerization degree was also noticed when toluene was used as reaction medium (DP=23) instead of molten bulk state (DP=47). These can be explained considering that the catalyst favored the simultaneous occurrence of more reactive sites in the molten bulk [40], while toluene prompted a higher mobility of reagents and thus more effective collisions. Consequently, both synthetic strategies promoted the obtaining of short chain lengths

[41]. The observation was important, suggesting the use of toluene as a suitable synthetic approach for grafting short PTMC chains on the chitosan backbones, avoiding the use of $Sn(Oct)_2$ toxic catalyst [42].

Applying the ring-opening polymerization of TMC on chitosan, the main difficulty was to reach a good contact between reagents in the absence of aprotic solvents, which can compete as initiators. This was a quite difficult task, considering the chitosan insolubility in aprotic solvents. The reaction in molten state proceeded in an insignificant percent at the chitosan sites. The explanation is obvious if it is considered that chitosan does not melt, and thus only a few reactive sites were available. The grafting proceeded well in toluene, which (i) prompted the chitosan's swelling and thus the enhancement of the number of available reactive sites [43] and (ii) favored the easy movement of TMC molecules to the reactive sites inside the swollen bulk chitosan. Water soluble products were obtained for a TMC/glucosamine molar ratio of 10 and 0.1, in the other cases the products were water insoluble (TMC/glucosamine = 5) or soluble in acidic water (TMC/glucosamine = 0.2). This indicated that the new derivatives' solubility was controlled by the PTMC chain length and the grafting degree on the chitosan backbones.

A question regarding the new PTMC-grafted-chitosan derivatives is: which reactive site could initiate the TMC polymerization? It was reported that ring-opening polymerization of TMC is initiated by compounds containing hydroxyl group, and also by different impurities from the reaction medium (e.g. water molecules) [36]. Nevertheless, some studies showed that the ring-opening polymerization of TMC and other cyclic carbonate derivatives can be initiated by amine containing compounds also [44]. To the best of our knowledge, no data about the competition between the hydroxyl and amine groups as initiators of ring-opening polymerization were reported so far. Considering that chitosan contains primary hydroxyl, secondary hydroxyl and amine groups, a competition between them as initiators may be anticipated. It is known that the nucleophilicity decreases as the electronegativity of the central atom increases, and thus the most susceptible for a nucleophilic attack should be the amine units. On the other hand, it is known that the bulkier a nucleophile is, the more difficult is to attack the substrate. In this literature context, the primary hydroxyl units could easier initiate the polymerization compared to amine or secondary hydroxyl groups which are sterically hindered because of their direct connection to the bulky D-glucosamine and *N*-acetyl-D-glucosamine rings. This hypothesis was supported by pH and conductometric measurements which indicated no significant change of the PTMC-grafted chitosan basicity compared to pristine chitosan (Figure S19-21). Consequently, it was assumed that the grafting reaction of

chitosan took place mainly at the primary hydroxyl units, as represented in Scheme 2. A hypothetic reaction mechanism has been drawn in Scheme 3.

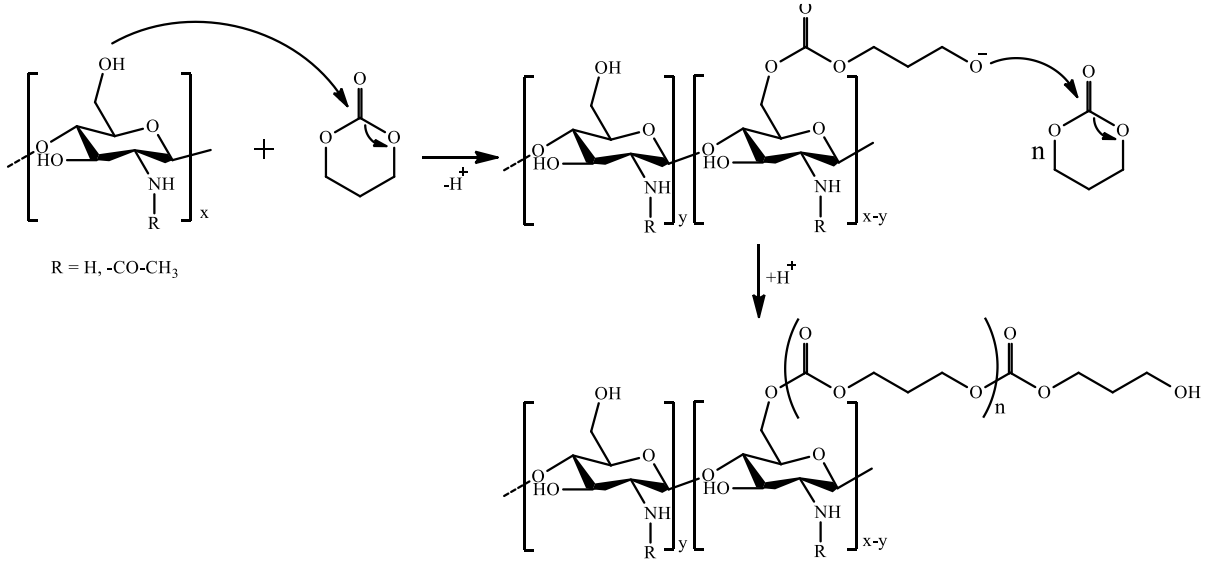

Scheme 3. The hypothetic reaction mechanism for the grafting of PTMC chains on chitosan

3.2 Solubility

Besides the investigation of a new synthetic route towards the obtaining of chitosan derivatives, the paper aimed to obtain new products with improved solubility, more suitable for *in vivo* applications. The solubility tests by visual observation indicated that **PC-10-T** and **PC-0.1-T** samples were water soluble for concentrations of 1% (Table 1, Figure 3). Moreover, **PC-10-T** was also soluble in DMSO, while **PC-5-T** and **PC-0.1-T** showed only partial solubility. Interestingly, in the less polar solvent, DMF, the solubility increased along with the decrease of PTMC content: **PC-0.1-T** showed partial solubility, **PC-5-T** swelled, while **PC-10-T** sample was completely insoluble. In the most polar solvent, methanol, all the samples were insoluble. It was concluded that the ratio between the hydrophilic chitosan/hydrophobic PTMC controlled the solubility of the final product. **PC-10-T** sample, which has good solubility in water and DMSO biodispersants, appears to be the most promising for further use in bio-applications.

Table 1. Solubility of some chitosan derivatives in water and common organic solvents

Sample	Water	DMF	DMSO	Methanol
Chitosan	-	-	-	-
PC-10-T	+	-	+	-
PC-5-T	-	***S***	±	-
PC-0.2-T	±	-	-	-
PC-0.1-T	+	±	±	±

+: soluble; -: insoluble; ±: partially soluble; **s**: swelling; The data were achieved by dissolving 10 mg sample into 1 mL solvent during 48 h, at 50° C.

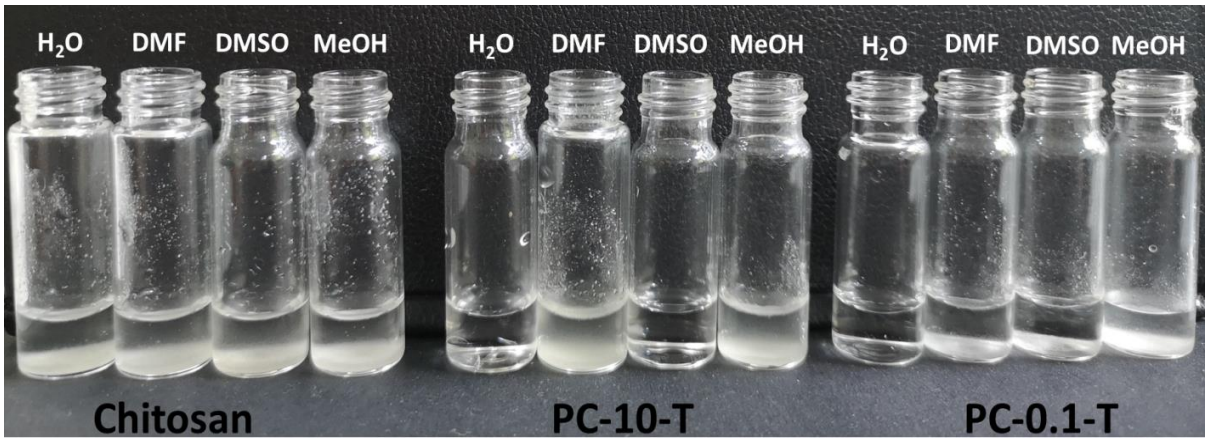

Figure 3. Visual assessment of the solubility of **Chitosan, PC-10-T** and **PC-0.1-T**

It is known that chitosan doesn't form real solutions, but colloidal ones due to the strong intra- and inter-molecular H-bonds, leading to coiled architectures [2]. To gain a deeper insight regarding the behavior in solution of the newly synthetized chitosan derivatives, the pH-dependent solubility was evaluated by measuring the solution transmittance at concentrations of 1 and 0.5 mg/mL [33]. As can be seen in Table 2, the solutions of **PC-10-T** and **PC-0.1-T** in neutral water have higher transmittance compared to the chitosan ones. Remarkable, their transmittance was higher even at the basic pH of 9, at the concentration of 0.5 mg/mL, clearly proving the solubility improvement on a larger pH range. However, while the solutions were macroscopic clear, the transmittance value indicated a turbidity degree. Deeper investigation by DLS revealed the presence of nano- and even micro-aggregates for all the studied samples, including the pristine chitosan, demonstrating that colloidal solutions were formed (Figure S22). The aggregates' dimension in the chitosan solution increased as the pH increased, according to the formation of coiled conformations in acidic pH because of intra- and inter-molecular H-bonds [2] and chitosan's precipitation in basic pH [45]. A similar trend was noticed for the PTMC-grafted-chitosan derivatives, but with significant lower diameter of the aggregates in the case of **PC-10-T**. This is explained by the presence of PTMC chains which, on one hand, favored the disruption of the inter-molecular H-bonds among the chitosan backbones, and, on the other hand, favored the self-assembling into aggregates by hydrophobic/hydrophilic segregation.

Table 2. Maximum transmittance of aqueous solutions of chitosan and chitosan derivatives

	Maximum transmittance (%)					
	Codes (solutions of 0.5 mg/mL)			**Codes (solutions of 1 mg/mL)**		
pH	**CS**	**PC-10-T**	**PC-0.1-T**	**CS**	**PC-10-T**	**PC-0.1-T**
3-4	85.39	79.12	86.14	89	68.64	82.59
7	63.36	70.6	88.03	60.13	75.3	83.31
8-9	64.02	70.75	68.19	60.47	51.66	40.23

3.3 Biocompatibility and biodegradability

The modification of chitosan raises questions regarding the alteration of its main properties, such as biocompatibility and biodegradability. To investigate them, *in vitro* biocompatibility and biodegradability tests were undertaken for the new derivatives compared to the pristine chitosan.

The biocompatibility was investigated for samples of different concentrations in contact with normal human dermal fibroblasts (NHDF) for 48 hours, by MTS assay, when reduction of cell viability by more than 30% was attributed to a cytotoxic effect, according to ISO 10993-5:2009(E) [46]. The results were given in Figure 4a and Figure S21. **PC-10-T** samples showed superior cell viability compared to the ones of chitosan for all the investigated concentrations. Thus, while the chitosan solutions showed biocompatibility for concentrations lower than 200 µg/mL, **PC-10-T** displayed good biocompatibility for concentrations lower than 300 µg/mL. Moreover, while all the cells died in contact with the 400 µg/mL chitosan solution, those in contact with **PC-10-T** of the same concentration showed a viability of almost 60%. No such effect was noticed in the case of **PC-0.1-T** sample. Even though **PC-0.1-T** toxicity was lower than that of chitosan at 25 µg/mL and 400 µg/mL, a higher cytotoxic effect was evident for the other concentrations. It is possible that the biocompatibility alteration of **PC-0.1-T** to be correlated with the formation of some supramolecular architectures by non-classical H-bonds indicated in the structural characterization step.

The obvious improvement of the **PC-10-T** biocompatibility compared to the chitosan one was mainly attributed to the better solubility in aqueous solutions, which circumvented the negative influence of acidity on cell viability. It should be mentioned that the improved solubility of **PC-10-T** allowed avoiding the use of any acid for solution's preparation. This is an importing finding, considering that many chitosan materials should be used in wet state, requiring the use of acids for their preparation (e.g. hydrogels). Besides, the presence of the hydrophobic, non-toxic PTMC chains could also participate to the biocompatibility

improvement [47]. Nevertheless, the biocompatibility determination on sample films showed no significant differences of NHDF cell viability, indicating the acetic acid used for chitosan's solution preparation as cytotoxic agent (Figure 4b).

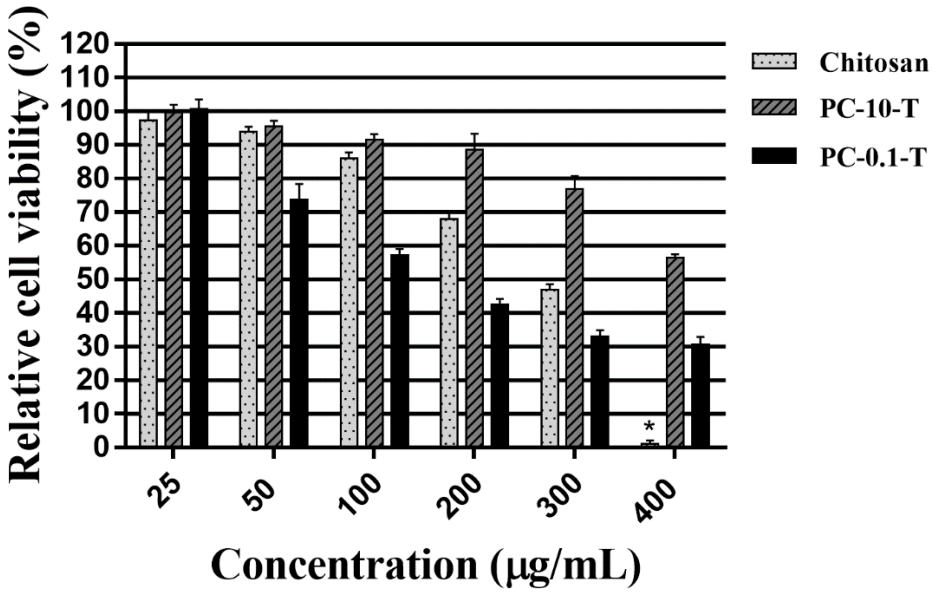

a)

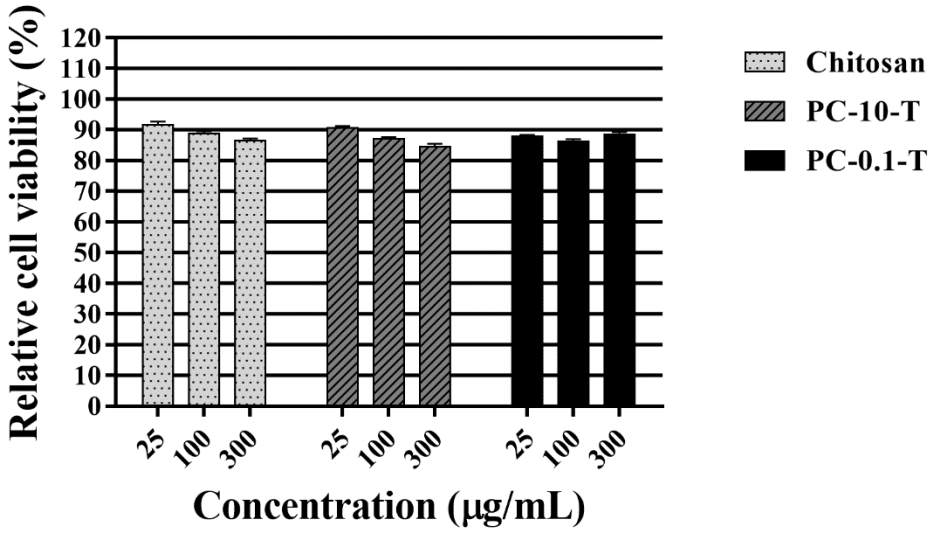

b)

Figure 4. Graphical representation of the relative cell viability of NHDF cells in contact for 48 hours with a) sample solutions of various concentrations, and b) film samples. The relative cell viability of treated cells is expressed as percentage of untreated cells viability. The results were presented as a mean value ± the standard error of the mean (S.E.M.), n = 8 for solution samples and n = 9 for film samples; * $p < 0.05$ for **Chitosan** vs. **PC-10-T** and **PC-0.1-T**, respectively, for tests on solution samples by two-way ANOVA using Dunnett's multiple comparisons test. The differences in cytotoxicity of films samples were not considered statistically significant.

Chitosan's biodegradation occurs under the influence of lysozyme, a human enzyme found in various body fluids, which has the ability to hydrolyze the glyosidic linkages of chitosan [48]. As chitosan is the main component of the synthetized derivatives, their biodegradability was investigated by enzymatic degradation tests in lysozyme buffer solution (pH=7.4), following the mass change of the samples after 21 days incubation period. Pristine chitosan showed a mass loss of 66%, similar to other reports [49], while **PC-10-T** reached a mass loss of 81%. The more advanced biodegradation of **PC-10-T** was attributed to its higher solubility at physiological pH, induced by grafting PTMC lateral chains on chitosan backbones. This hypothesis was supported by SEM images recorded on the samples before and after degradation (Figure 5). They indicated a surface erosion process of the samples on the out-in direction, reached by degradation/dissolution processes.

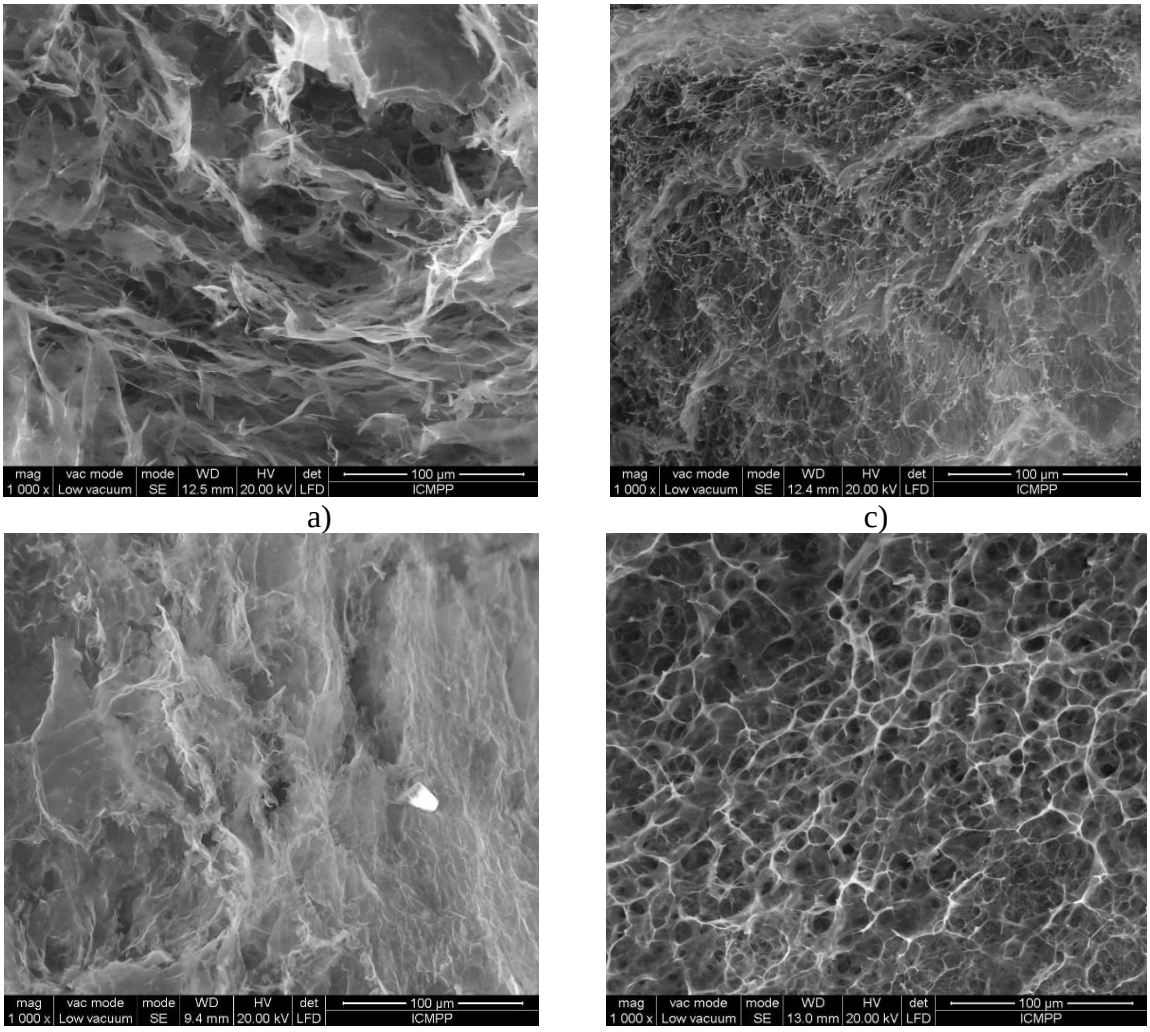

Figure 5. SEM images of (a, b) **chitosan** and (c, d) **PC-10-T** samples, before and after enzymatic degradation process (magnification 1000x)

3.4 Morphology and surface characterization

For *in vivo* applications, the ordering degree and the surface of materials is of major importance, a nanostructured surface being beneficial for cell growth [50]. To see how the PTMC grafting altered the surface properties of chitosan, the films casted from aqueous solutions were observed by polarized optical microscopy (POM) and atomic force microscopy (AFM). POM images indicated strong birefringence with fine granular texture for the chitosan films (Figure 6a), in agreement with its semicrystalline nature [51]. No significant modification of this texture was observed for the grafted chitosan derivative **PC-10-T** (Figure 6b). However, a careful analysis of the images revealed richer details resulting in clearer textures in the case of PTMC-grafted-chitosan derivatives (inserts of Figure 6). Considering that the semicrystalline nature of chitosan is given by the ordering of chain segments into clusters, it can be assessed that the texture clarification for the **PC-10-T** sample was the result of a more precise self-ordering guided by its amphiphilic structure. This was somehow indicated by the DLS measurements, which showed smaller nano-aggregates for the PTMC-grafted-chitosan aqueous solutions compared to pristine chitosan ones.

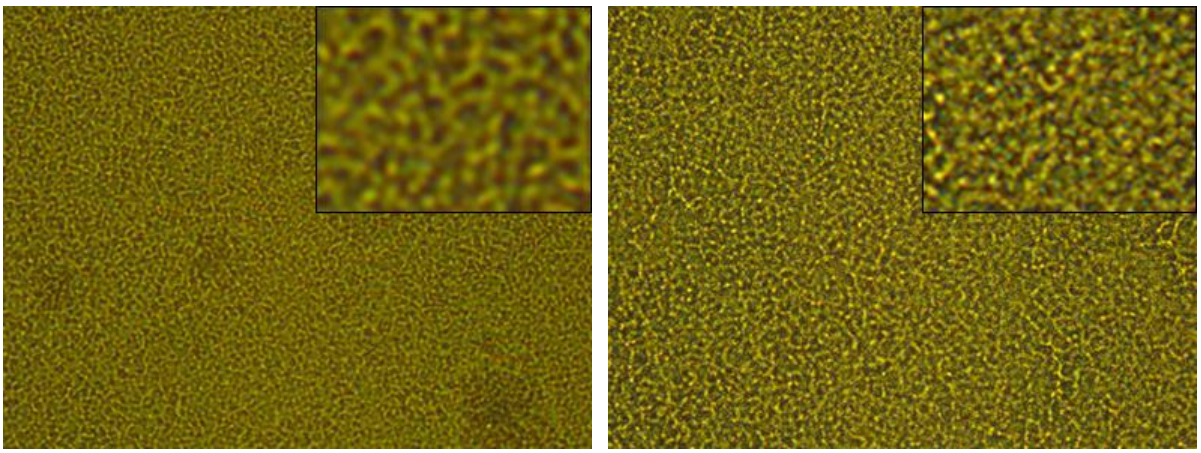

a) **b)**

Figure 6. POM images of a) **chitosan**, and b) **PC-10-T** films casted from aqueous solutions

A deeper insight on the ordering influence on film surface was gained by atomic force microscopy. The three-dimensional (3D) images revealed a granular morphology for all samples, with sub-micrometric grains (Figure 7, Figure S23). Nevertheless, the roughness average (R.a.) had values lower than 30 nm, which is favorable for cell growth [52]. Moreover, the calculation of the roughness exponent (R.E.) showed values lower than 1, in accordance with a bi-dimensional surface [53, 54]. No significant differences were observed between the surface parameters of the pristine chitosan and of the studied derivatives, demonstrating that the PTMC grafting did not significantly influence them (Table 4).

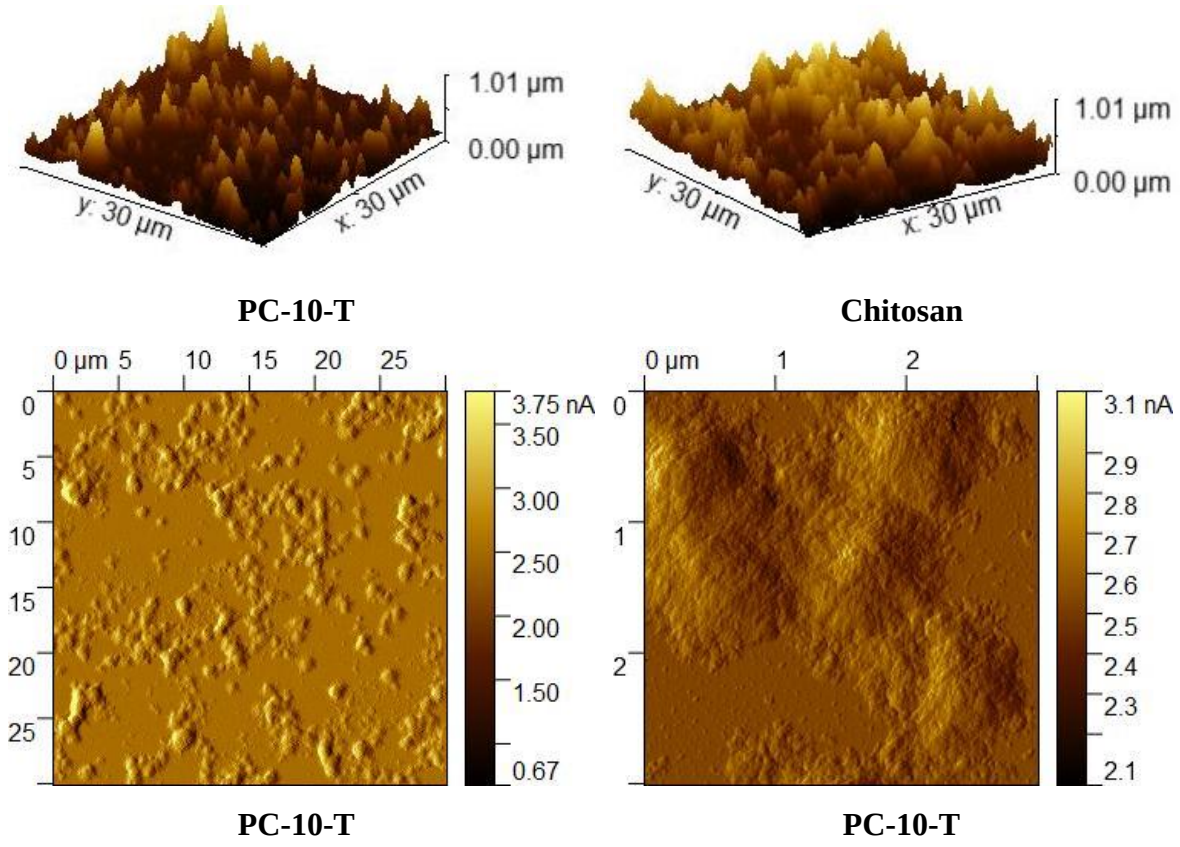

Figure 7. Representative AFM images for chitosan and **PC-10-T**

An important parameter regarding biomaterials which affects their *in vivo* application is the wettability, quantified by water contact angle. Chitosan films have the contact angle around 100º, higher than the superior limit of the moderate hydrophilicity range (60 - 90º domain), which is the most favourable for cell adhesion [55, 56]. The rather hydrophobic character of its films is attributed to the strong intra- and inter-molecular H-bonds developed between the hydroxyl groups, exposing the hydrophobic backbones to the film surface.

Interesting enough, the water-to-air contact angle of the PTMC-grafted-chitosan films showed lower values, lying in the moderate hydrophilicity range (Table 4). The improved hydrophilicity of the PTMC-grafted-chitosan films can be explained considering their behaviour in solution. DLS measurements demonstrated the formation of colloidal solutions due to aggregation. It is expected that the amphiphilic character of the PTMC-grafted-chitosan polymers in aqueous solutions to guide the self-assemble with the PTMC chains into the central part forming a hydrophobic core and the chitosan chains at the edge. Thus, while the chitosan aggregates generated by the inter- and intra- molecular H-bonds shielded the hydrophilic hydroxyl units into an H-bonding network [2], the PTMC-grafted-chitosan aggregates exposed

the chitosan chains to the edge, with free hydrophilic hydroxyl groups. In such a way, the grafting of PTMC proved to be beneficial for the improving of the film's surface hydrophilicity.

Table 4. Roughness average, roughness exponent and water contact angle of the synthetized chitosan derivatives

Sample	R.a. (30x30)	R.E.	Water mean contact angle ± S.D.(º)
Chitosan	22.363	0.511	103.8±1.96
PC-10-T	35.172	0.914	66.41±3.11
PC-0.2-T	7.057	0.135	86.89±2.24
PC-0.1-T	20.193	0.429	63.57±2.43

R.a. measured for surfaces of 30x30 cm^2; R.E. roughness exponent calculated as the slope of roughness versus scan size, in a double log plot.

Conclusions

New amphiphilic chitosan derivatives were synthetized by ring-opening polymerization of 1,3-dioxan-2-one (trimethylene carbonate) initiated by functional groups of chitosan. Good solubility in water and DMSO biodispersants was reached for a grafting degree around 5% of chitosan with poly(trimethylene carbonate) chains having a polymerization degree around 7. The water solubility allowed to avoid the use of acids for solution preparation, improving the biocompatibility of the poly(trimethylene carbonate) in wet state, a cell viability value of ~80% compared to less than 50% for chitosan being recorded for solutions of concentration of 300 µg/mL. The improved solubility of the new synthetized chitosan derivatives prompted a higher biodegradation rate, 81% mass loss compared to 66% for pristine chitosan in 21 days. Moreover, the grafting proved to be beneficial for the hydrophilicity improvement of the films casted from aqueous solutions. It was concluded that poly(trimethylene carbonate) grafted chitosan is a valuable biopolymer for *in vivo* applications, further studies for biomaterials' preparation such as hydrogels and nanofibers being in progress.

Acknowledgements

The research leading to these results has received funding from the Romanian National Authority for Scientific Research, MEN-UEFISCDI grant, project number RO-NO-2019-0540 (no. 14/2020).

References

1. M.N.V.R. Kumar, A review of chitin and chitosan applications, React. Funct. Polym. 46 (2000) 1-27. DOI: 10.1016/S1381-5148(00)00038-9.

2. M. Rinaudo, Chitin and chitosan: Properties and applications, Prog. Polym. Sci. 31 (2006) 603-632. DOI: 10.1016/j.progpolymsci.2006.06.001.

3. M. Dash, F. Chiellini, R.M. Ottenbrite, E. Chiellini, Chitosan - a versatile semi-synthetic polymer in biomedical applications, Prog. Polym. Sci. 36 (2011) 981-1014. DOI: 10.1016/j.progpolymsci.2011.02.001.

4. P.S. Bakshi, D. Selvakumar, K. Kadirvelu, N.C. Kumar, Chitosan as an environment friendly biomaterial - a review on recent modifications and applications, Int. J. Biol. Macromol. 150 (2020) 1072-1083. DOI: 10.1016/j.ijbiomac.2019.10.113.

5. D. Ailincai, W. Porzio, L. Marin, Hydrogels Based on Imino-Chitosan Amphiphiles as a Matrix for Drug Delivery Systems, Polymers 12 (2020) 2687. DOI: 10.3390/polym12112687.

6. A.M. Craciun, L. Mititelu-Tartau, M. Pinteala, L. Marin, Nitrosalicyl-imine-chitosan hydrogels based drug delivery systems for long term sustained release in local therapy, J. Colloid Interface Sci. 536 (2019) 196-207. DOI:10.1016/j.jcis.2018.10.048.

7. L. Marin, M. Popa, A. Anisiei, S.A. Irimiciuc, M. Agop, T.C. Petrescu, D. Vasincu, L. Himiniuc, A theoretical model for release dynamics of an antifungal agent covalently bonded to the chitosan, Molecules 2021, 26, 2089. DOI: doi.org/10.3390/molecules26072089.

8. A.G. Rusu, A.P. Chiriac, L.E. Nita, I. Rosca, D. Rusu, I. Neamtu, Self-assembled nanocarriers based on modified chitosan for biomedical applications: Preparation and characterization, Polymers 2020, 12(11), 2593. DOI: doi.org/10.3390/polym12112593.

9. S. Xiong, L. Marin, L. Duan, X. Cheng, Fluorescent chitosan hydrogel for highly and selectively sensing of p-nitrophenol and 2, 4, 6-trinitrophenol, Carbohydr. Polym. 225 (2019) 115253. DOI: 10.1016/j.carbpol.2019.115253.

10. C.A. Ghiorghita, K.B.L. Borchert, A.L. Vasiliu, M. M. Zaharia, D. Schwarz, M. Mihai, Porous thiourea-grafted-chitosan hydrogels: Synthesis and sorption of toxic metal ions from contaminated waters, Colloid Surface A. 607 (2020) 125504. DOI: 10.1016/j.colsurfa.2020.125504.

11. A. Bejan, F. Doroftei, X. Cheng, L. Marin, Phenothiazine-chitosan based eco-adsorbents: A special design for mercury removal and fast naked eye detection, Int. J. Biol. Macromol. 162 (2020) 1839-1848. DOI: 10.1016/j.ijbiomac.2020.07.232.

12. M.M. Iftime, G.L. Ailiesei, E. Ungureanu, L. Marin, Designing chitosan based eco-friendly multifunctional soil conditioner systems with urea controlled release and water retention, Carbohydr. Polym. 223 (2019) 115040. DOI: 10.1016/j.carbpol.2019.115040
13. Y. Wu, A. Rashidpour, M.P. Almanjo, I. Metón, Chitosan-Based Drug Delivery System: Applications in Fish Biotechnology, Polymers 12 (2020) 1177. DOI: 10.3390/polym12051177
14. C. Branca, G. D'Angelo, C. Crupi, K. Khouzami, S. Rifici, G. Ruello, U. Wanderlingh, Role of the OH and NH vibrational groups in polysaccharide-nanocomposite interactions: A FTIR-ATR study on chitosan and chitosan/clay films, Polymer, 99 (2016) 614–622. DOI: 10.1016/j.polymer.2016.07.086.
15. R.M. El-Shishtawy, S.A. Mohamed, A.M. Asiri, N.S.E. Ahmed, Synthesis of hemicyanine-based chitosan ligands in dye-affinity chromatography for the purification of chewing stick peroxidase, Int. J. Biol. Macromol. 148 (2020) 401-414. DOI: 10.1016/j.ijbiomac.2020.01.088
16. Q. Zia, M. Tabassum, J. Meng, Z. Xin, H. Gong, J. Li, Polydopamine-assisted grafting of chitosan on porous poly (L-lactic acid) electrospun membranes for adsorption of heavy metal ions, Int. J. Biol. Macromol. 167 (2021) 1479-1490. DOI: 10.1016/j.ijbiomac.2020.11.101
17. W.Tan, J. Zhang, Y. Mi, F. Dong, Q. Li, Z. Guo, Enhanced antifungal activity of novel cationic chitosan derivative bearing triphenylphosphonium salt via azide-alkyne click reaction, Int. J. Biol. Macromol. 165 (2020) 1765-1772. DOI: 10.1016/j.ijbiomac.2020.10.019.
18. L. Marin, B. Dragoi, N. Olaru, E. Perju, A. Coroaba, F. Doroftei, G. Scavia, S. Destri, S. Zappia, W. Porzio, Nanoporous furfuryl-imine-chitosan fibers as a new pathway towards ecomaterials for CO2 adsorption, Eur. Polym. J. 120 (2019) 109214. DOI: doi.org/10.1016/j.eurpolymj.2019.109214
19. C. Stefanescu, W.H. Daly, I.I. Negulescu, Functionalization of cellulose and chitosan in ionic liquids, Cellulose Chem. Technol. 54 (2020) 857-868. DOI: 10.35812/CelluloseChemTechnol.2020.54.84.
20. B. Fonseca-Santos, M. Chorilli, An overview of carboxymethyl derivatives of chitosan: their use as biomaterials and drug delivery systems, Mater. Sci. Eng. C 77 (2017) 1349–1362. DOI:10.1016/j.msec.2017.03.198.
21. R. Yu, L.C. de Saint-Cyr, L. Soussan, M. Barboiu, S. Li, Anti-bacterial dynamic hydrogels prepared from O-carboxymethyl chitosan by dual imine bond crosslinking for biomedical applications, Int. J. Biol. Macromol. 167 (2021) 1146-1155. DOI: 10.1016/j.ijbiomac.2020.11.068.

22. L. Gabriel, A. Tied, T. Heinze, Carboxymethylation of polysaccharides – a comparative study, Cell. Chem. Technol. 54 (2020) 835-844. DOI: 10.35812/CelluloseChemTechnol.2020.54.82

23. S. Dimassi, N. Tabary, F. Chai, N. Blanchemain, B. Martel, Sulfonated and sulfated chitosan derivatives for biomedical applications: A review, Carbohydr. Polym. 202 (2018) 382-396. DOI:10.1016/j.carbpol.2018.09.011.

24. R. Cheung, R. Ng, J. Wong, W. Chan, Chitosan: an update on potential biomedical and pharmaceutical applications, Mar. Drugs 13 (2015) 5156–5186. DOI:10.3390/md13085156.

25. I. Bravoosuna, D. Teutonico, S. Arpicco, C. Vauthier, G. Ponchel, Characterization of chitosan thiolation and application to thiol quantification onto nanoparticle surface, Int. J. Pharm. 340 (2007) 173–181. DOI:10.1016/j.ijpharm.2007.03.019.

26. R. Jayakumar, N. Selvamurugan, S.V. Nair, S. Tokura, H. Tamura, Preparative methods of phosphorylated chitin and chitosan—An overview, Int. J. Biol. Macromol. 43 (2008) 221–225. DOI: 10.1016/j.ijbiomac.2008.07.004.

27. B.I. Andreica, X. Cheng, L. Marin, Quaternary ammonium salts of chitosan. A critical overview on the synthesis and properties generated by quaternization, Eur. Polym. J. 139 (2020) 110016. DOI:10.1016/j.eurpolymj.2020.110016.

28. Z. Shariatinia, Carboxymethyl chitosan: Properties and biomedical applications, Int. J. Biol. Macromol, 120 (2018) 1406–1419. DOI:10.1016/j.ijbiomac.2018.09.131.

29. W. Wang, Q. Meng, Q. Li, J. Liu, M. Zhou, Z. Jin, K. Zhao, Chitosan derivatives and their application in biomedicine, Int. J. Mol. Sci. 21(2) (2020) 487. DOI:10.3390/ijms21020487.

30. Z. Zhang, R. Kuijer, S.K. Bulstra, D.W. Grijpma, J. Feijen, The in vivo and in vitro degradation behavior of poly(trimethylene carbonate), Biomaterials 27 (2006) 1741-1748. DOI: 10.1016/j.biomaterials.2005.09.017.

31. K. Fukushima, Poly(trimethylene carbonate)-based polymers engineered for biodegradable functional biomaterials, Biomater. Sci. 4 (2016) 9-24. DOI: 10.1039/C5BM00123D

32. T.V. Shah, D.V. Vasava, A glimpse of biodegradable polymers and their biomedical applications, e-Polymers 19 (2019) 385–410. DOI: 10.1515/epoly-2019-0041

33. R.J. Verheul, M. Amidi, S. van der Wal, E. van Riet, W. Jiskoot, W.E. Hennink, Synthesis, characterization and in vitro biological properties of O-methyl free *N*,*N*,*N*-trimethylated chitosan, Biomaterials, 29 (2008) 3642–3649. doi:10.1016/j.biomaterials.2008.05.026.

34. S.M. Lim, D.K. Song, S.H. Oh, D.S. Lee-Yoon, E.H. Bae, J.H. Lee, In vitro and in vivo degradation behavior of acetylated chitosan porous beads. J. Biomater. Sci. Polym. Ed., 19 (2008) 453–466. DOI:10.1163/156856208783719482.

35. F. Yu, R. Zhuo, Synthesis and characterization of OH-Terminated Poly(trimethylene carbonate)s by alcohol-initiated ring-opening polymerization in melt bulk without using any catalyst, Polym. J. 36 (2004) 28–33. DOI:10.1295/polymj.36.28

36. D. Delcroix, B. Martín-Vaca, D. Bourissou, C. Navarro, Ring-Opening Polymerization of Trimethylene Carbonate catalyzed by methanesulfonic acid: activated monomer versus active chain end mechanisms, Macromolecules, 43 (2010) 8828–8835. DOI:10.1021/ma101461y.

37. L. Marin, S. Shova, C. Dumea, E. Bicu, D. Belei, Self-assembled Triazole AIE-Active Nanofibers: Synthesis, Morphology, and Photophysical Properties, Cryst. Growth Des. 17 (2017) 3731–3742. DOI: 10.1021/acs.cgd.7b00351.

38. P.E. Hansen, J. Spanget-Larsen, NMR and IR investigations of strong intramolecular hydrogen bonds, Molecules 22 (2017) 552. DOI:10.3390/molecules22040552.

39. S. Zhou, L. Wang, Symmetry and ^{1}H NMR chemical shifts of short hydrogen bonds: impact of electronic and nuclear quantum effects, Phys. Chem. Chem. Phys. 22 (2020) 4884-4895. DOI: 10.1039/C9CP06840F.

40. A.P. Pêgo, Z. Zhong, P.J. Dijkstra, D.W. Grijpma, J. Feijen, Influence of catalyst and polymerization conditions on the properties of 1,3-Trimethylene Carbonate and Ɛ-Caprolactone copolymers, Macromol. Chem. Phys. 204(56) (2003) 747–754. DOI: 10.1002/macp.200390043.

41. S. Penczek, J. Pretula, S. Slomkowski, Ring-opening polymerization, Chemistry Teacher International, (2021). DOI: 10.1515/cti-2020-0028.

42. M.C. Tanzi, P. Verderio, M.G. Lampugnani, M. Resnati, E. Dejana, E. Sturani, Cytotoxicity of some catalysts commonly used in the synthesis of copolymers for biomedical use, J. Mater. Sci. Mater. Med. 5(6-7) (1994) 393–396. DOI:10.1007/bf00058971.

43. L. Liu, Y. Wang, X. Shen, Y. Fang, Preparation of chitosan-g-polycaprolactone copolymers through ring-opening polymerization of ε-caprolactone onto phthaloyl-protected chitosan, Biopolymers, 78(4) (2005) 163–170. DOI:10.1002/bip.20261.

44. W.N. Ottou, H. Sardon, D. Mecerreyes, J. Vignolle, D. Taton, Update and challenges in organo-mediated polymerization reactions, Prog. Polym. Sci. 56 (2016) 64–115. DOI:10.1016/j.progpolymsci.2015.12.001.

45. M.I. Wahba, Sodium bicarbonate-gelled chitosan beads as mechanically stable carriers for the covalent immobilization of enzymes, Biotechnol. Prog. 34 (2018) 347–361. DOI:10.1002/btpr.2587.

46. ISO, Biological evaluation of medical devices – Part 5: Tests for in vitro cytotoxicity Title, (2009).].

47. K. Fukushima, Poly(trimethylene carbonate)-based polymers engineered for biodegradable functional biomaterials, Biomater. Sci., 4 (2016) 9–24. DOI:10.1039/C5BM00123D.
48. S. Hirano, Y. Yagi, The effects of N-substitution of chitosan and the physical form of the products on the rate of hydrolysis by chitinase from *Streptomyces griseus*, Carbohydr. Polym. 83(1) (1980) 103-108. DOI: 10.1016/S0008-6215(00)85369-0.
49. I. Zainol, S.M. Ghani, A. Mastor, M.A. Derman, M.F. Yahya, Enzymatic degradation study of porous chitosan membrane. Mater. Res. Innov, 13(3) (2009) 316–319. DOI:10.1179/143307509x440631.
50. L. Richert, F. Vetrone, J.H. Yi, S.F. Zalzal, J.D. Wuest, F. Rosei, A. Nanci, Surface nanopatterning to control cell growth, Adv. Mater. 20(8) (2008) 1488–1492. DOI:10.1002/adma.200701428.
51. F. Croisier, C. Jérôme, Chitosan-based biomaterials for tissue engineering, Eur. Polym. J. 49(4) (2013) 780–792. DOI:10.1016/j.eurpolymj.2012.12.009.
52. R.C.C. Wang, M.C. Hsieh, T.M. Lee, Effects of nanometric roughness on surface properties and fibroblast's initial cytocompatibilities of Ti6AI4V, Biointerphases 6 (2011) 87. DOI: 10.1116/1.3604528.
53. J. Macanás, L. Palacio, P. Prádanos, A. Hernandez, M. Munoz, Atomic force microscopy as a suitable technique for surface characterization of activated composite membranes for metal ion facilitated transport, Appl. Phys. A 84 (2006) 277–284. DOI:10.1007/s00339-006-3609 -x.
54. L. Marin, D. Timpu, V. Cozan, G.I. Rusu, A. Airinei, Solid state properties of thin films of new copoly(azomethine-sulfone)s, J. Appl. Polym. Sci. 120(3) (2010) 1720–1728. DOI:10.1002/app.33313.
55. Y. Ikada, Surface modification of polymers for medical applications, Biomaterials 15 (1994) 726–736. DOI:10.1016/0142-9612(94)90025-6.
56. L. Marin, D. Ailincai, M. Mares, E. Paslaru, M. Cristea, V. Nica, B.C. Simionescu, Imino-chitosan biopolymeric films. Obtaining, self-assembling, surface and antimicrobial properties, Carbohydr. Polym. 117 (2015) 762–770. DOI:10.1016/j.carbpol.2014.10.050.